

dvancing III-phosphide red light-emitting diode performance through ternary and graded ternary electron blocking layer

Anum, Muhammad Usman, Usman Habib, and Shazma Ali

Citation: Chin. Phys. B, 2026, 35 (**4**): 044205. DOI: 10.1088/1674-1056/ae0639
http://cpb.iphy.ac.cn; http://iopscience.iop.org/cpb

What follows is a list of articles you may be interested in

Ultrafast charging quantum battery with cavity-cavity interactions

Zhuoheng Wang(王卓恒), Zefeng Huang(黄泽丰), Dayang Zhang(张大洋), Yu Zhao(赵愈), Youbin Yu(俞友宾), Guangri Jin(金光日), and Aixi Chen(陈爱喜)
Chin. Phys. B, 2026, 35 (**3**): 034204. DOI: 10.1088/1674-1056/adfef9

Thermally managed ring-cavity design enables LED-pumped Nd,Ce:YAG continuous wave single-longitudinal-mode laser for cost-effective precision photonics

Rong-Rong Jiang(江容容), Rui-Ze Xia(夏瑞泽), Feng-Yang Xing(邢凤阳), Liang Chen(陈亮), Yang Chen(陈阳), Feng-Bo Zhang(张峰博), Huan-Yu Zuo(左环宇), Jian-Ping Shen(沈建平), and Ling-Hai Xie(解令海)
Chin. Phys. B, 2026, 35 (**3**): 034203. DOI: 10.1088/1674-1056/adfbd5

Full stabilization of eight-channel Yb-fiber coherent beam combining system delivering 1.18-kW, 1.18-mJ, 270-fs pulses

Zhuo Shi(史卓), Zhi-Hang Du(杜志航), Cheng-Bin Liang(梁成斌), Hong-Xiang Chang(常洪祥), Zi-Kai Dong(董自凯), Hong-Yu Guo(郭鸿宇), Can Li(李灿), Pu Zhou(周朴), Zhi-Yi Wei(魏志义), and Guo-Qing Chang(常国庆)
Chin. Phys. B, 2026, 35 (**2**): 024210. DOI: 10.1088/1674-1056/ae1952

Controllable phase-dependent optical switch in an atom-cavity system

Xu-Yang Li(李旭阳), Yuan-Feng Lu(陆元峰), Ya-Jie Wu(吴亚杰), Ning Li(荔宁), and Miao-Di Guo(郭苗迪)
Chin. Phys. B, 2026, 35 (**2**): 024205. DOI: 10.1088/1674-1056/adfc40

Output light power of InGaN-based violet laser diodes improved by using a u-InGaN/GaN/AlGaN multiple upper waveguide

Feng Liang(梁锋), De-Gang Zhao(赵德刚), De-Sheng Jiang(江德生), Zong-Shun Liu(刘宗顺), Jian-Jun Zhu(朱建军), Ping Chen(陈平), Jing Yang(杨静), Wei Liu(刘炜), Shuang-Tao Liu(刘双韬), Yao Xing(邢瑶), Li-Qun Zhang(张立群), Wen-Jie Wang(王文杰), Mo Li(李沫), Yuan-Tao Zhang(张源涛), Guo-Tong Du(杜国同)
Chin. Phys. B, 2017, 26 (**12**): 124210. DOI: 10.1088/1674-1056/26/12/124210

Advancing III–phosphide red light-emitting diode performance through ternary and graded ternary electron blocking layer

Anum, Muhammad Usman[†], Usman Habib, and Shazma Ali

Faculty of Engineering Sciences, Ghulam Ishaq Khan Institute of Engineering Sciences and Technology, Topi, Swabi, Khyber Pakhtunkhwa, Pakistan

(Received 11 July 2025; revised manuscript received 9 September 2025; accepted manuscript online 12 September 2025)

Gallium indium phosphide (GaInP)/aluminum gallium indium phosphide (AlGaInP) red-emitting active region has been numerically employed and investigated in III–V light-emitting diodes (LEDs) in this work. We have employed ternary aluminum gallium phosphide (AlGaP) electron blocking layer (EBL) and graded AlGaP EBL (or GEBL) separately in the red-emitting LED. According to the simulation results, improvements in internal quantum efficiency (IQE), radiative recombination rate ($R_{\rm rad}$), and carrier concentrations have been observed. Up to 9% decrease in efficiency droop is observed in red-emitting LEDs with ternary EBLs. Good carrier confinement has resulted in high $R_{\rm rad}$ and, thus, increased optical output. The proposed EBLs may, thus, be adopted due to their high optical output in red-emitting LEDs, particularly for high current applications.

Keywords: III–phosphide, electron blocking layer, efficiency, red emission, light-emitting diode, radiative recombination

PACS: 42.60.Lh, 71.55.Eq, 78.60.–b, 85.60.Bt

DOI: 10.1088/1674-1056/ae0639 **CSTR:** 32038.14.CPB.ae0639

1. Introduction

III–phosphide LEDs, especially AlGaInP-based LEDs, are essential in many fields, including automotive electronics, illumination, display technologies, and medical therapies.[1–3] AlGaInP is a direct bandgap semiconductor with an energy bandgap tunable from approximately 1.8 eV to 2.3 eV. Although the bandgap energy of AlGaInP can reach $\sim$ 2.3 eV (green light), LED efficiency drops sharply in the green-yellow and green regions due to the band structure becoming less "direct-like" at higher aluminum concentrations.[3,4] With peak internal quantum efficiency reaching 99%, AlGaInP-based red LEDs exhibit exceptional photon conversion, with the emitted wavelength determined by the quaternary AlGaInP alloy composition.[3,5–7] To emit longer wavelengths (i.e., $>$ 650 nm), AlGaInP heterostructure LEDs need a compressive strain of over 1% in the GaInP active layer. However, the resulting lattice mismatch causes defects that affect growth and device properties.[8] Due to low p-type conductivity, AlGaInP devices require large current-spreading layers, which can be difficult to achieve. It is challenging to confine electrons in the emission layer due to the relatively low electron confinement potential provided by AlInP. Asymmetric p–n junction-induced carrier loss has been identified as the reason of efficiency droop observed in AlGaInP LEDs at low current levels[9] An extensive analysis of the internal quantum efficiency (IQE) of red and amber AlGaInP LEDs has determined that the leakage is caused by insufficient barrier heights dividing QWs in the active region.[10] At high injection current levels, p-side electron leakage has also been reported to be the cause of efficiency droop in AlGaInP LEDs.[11–14] To address these challenges, numerous potential solutions have been suggested by researchers such as the utilization of optimum quantum well counts[15] and the use of a tensile strain barrier layer.[16] Quaternary InGaAlP EBL in InGaP/InGaAlP multiquantum well red RCLEDs has also been presented.[17] AlGaP quantum barriers have also been explored in the literature.[18] EBL engineering has also been reported to address these challenges.[19] Furthermore, thermal analysis of InGaP/InGaAlP multiquantum well LEDs has been explored in several studies.[20–23]

In this work, we integrate AlGaP EBL and graded AlGaP EBL into traditional red-emitting LEDs. We numerically analyze the effect of AlGaP EBLs on the optoelectronic characteristics of red-emitting LEDs. To the best of our knowledge, AlGaP EBLs have not been explored in GaInP/AlGaInP quantum well LEDs. AlGaP lattice compatibility, and band alignment characteristics make it a promising choice as an electron blocking layer in AlGaInP-based LEDs. We believe our results are experimentally reproducible because AlGaInP/GaInP multi-quantum well (MQW) LEDs have been successfully grown using MOCVD.[24] Moreover, linearly-graded AlGaInP have been successfully grown using MBE.[25] Additionally, AlGaP morphology has been investigated using MBE in Ref. [26].

[†]Corresponding author. E-mail: usmanishfaq@yahoo.com

© 2026 Chinese Physical Society and IOP Publishing Ltd. All rights, including for text and data mining, AI training, and similar technologies, are reserved.

2. Device structure and parameters

We numerically analyze three LEDs, i.e., LED M1, LED M2, and LED M3, which are displayed in Fig. 1. The LED M1 is adapted from Refs. [27,28]. In this design, the substrate is 300-nm thick and composed of n-GaAs. The n-region is made up of 750-nm thick n-$Al_{0.5}In_{0.5}P$. The active region comes after the n-region, which has fifteen QWs $Ga_{0.46}In_{0.54}P$ whose thickness is 8 nm, sandwiched between the sixteen $Al_{0.25}Ga_{0.20}In_{0.55}P$ quantum barriers whose thickness is 15 nm.[24,29,30] The dislocation density for such devices is reported to be 1×10^7 cm^{-2}.[31] The dimensions of the LED design are 200 μm ×400 μm. The p-region is made up of 750-nm thick p-$Al_{0.5}In_{0.5}P$. The LED M2 is like the LED M1 except a ternary $Al_{0.55}Ga_{0.45}P$ EBL of 15 nm to be used as shown in Fig. 1. The third structure LED M3 has a graded AlGaP EBL, in which aluminum is linearly graded between 0.55 to 0.95, accordingly. The graded EBL is 15-nm thick. We employ SiLENSe^{TM} 6.5.1 simulator for the numerical analysis of our red-emitting LEDs. The simulator employs Poisson–Schrödinger and $k \cdot p$ models to simulate the optoelectronic properties of III–V LEDs and LDs.[32] The electron mobility and the hole mobility of 800 cm^2/V·s and 141 cm^2/V·s are used respectively. The doping concentrations in p-AlInP and n-AlInP are 5×10^{17} cm^{-3} and 1×10^{18} cm^{-3}.[33] The three conduction-band valleys (Γ, X, and L) in AlGaInP are taken into account for the analysis.[27,32,34] Recombination lifetime is 1×10^{-8} (in unit of s), the Auger coefficient is 1×10^{-30} (in units of cm^6/s), the radiative recombination coefficient is 1.44×10^{-10} (in units of cm^3/s), and the band offset ratio is 0.65/0.35. Some of the known limitations of the widely used models utilized in the numerical simulation of LEDs include assumption of continuous charge distribution, which may not accurately represent the localized charge trapping or discrete energy states. In the regions of strong electric fields, additional corrections may be needed to account for nonlinear effects. The models do not fully capture carrier screening effects, which can impact recombination rates and efficiency. Additionally, in strained quantum well structures, spontaneous and piezoelectric polarization effects can complicate self-consistent calculations.[27,35] The voltage range to study the characteristics of the LEDs is set to 1 V–5 V.

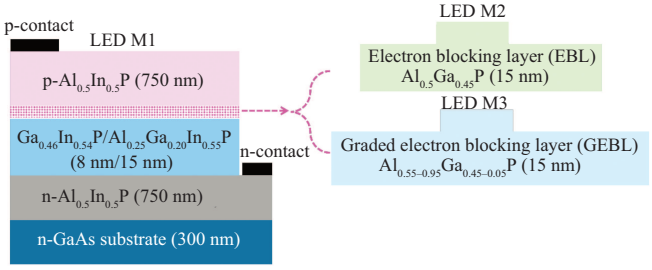


Fig. 1. Schematics diagram of LED M1, LED M2, and LED M3.

3. Results and discussion

The internal quantum efficiency (IQE) is computed numerically by summing up the radiative contributions from all QWs in the whole active region using the relation

$$\mathrm{IQE} = \frac{Q}{J} \int R_{\mathrm{rad}}, \tag{1}$$

where J is the current density and Q is the charge. Figure 2(a) illustrates the IQE of LED M1, LED M2, and LED M3. The electrons and holes enter MQWs from the n- and p-sides respectively where radiative carrier recombination produces the IQE. The comparatively greater radiative recombination rate of LED M3 accounts for its improved IQE, according to Eq. (1). Compared to LED M1 and LED M2, LED M3 (with graded AlGaP EBL) exhibits a higher peak efficiency with significantly less droop. Up to 9% decrease in efficiency droop is observed in red-emitting LEDs with ternary AlGaP EBLs. The improved optoelectronic features of LED M2 and LED M3 are attributed to the AlGaP EBL in LED M2, and GEBL in LED M3.

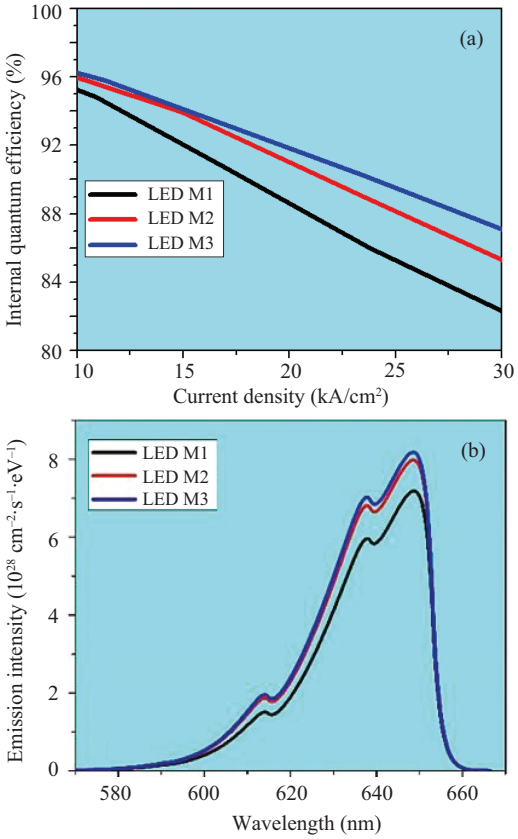


Fig. 2. (a) The internal quantum efficiency and (b) the emission intensity at 3 kA/cm^2 of LED M1, LED M2, and LED M3.

Figure 2(b) displays the emission intensity graph of LED M1, LED M2, and LED M3 at a current density of 3 kA/cm^2. Such high current densities for GaInP/AlGaInP quantum wells have been reported.[21,36] The emission spectra demonstrate that each LED is emitting in the red range with a peak at ∼ 650 nm. In the same manner, emission broadening

is noted in LED M2 and LED M3. LED M3 has the highest peak emission intensity among other LEDs. This is due to the comparatively reduced asymmetric distribution of carriers and enhanced overlapping of the electron–hole wavefunction in the active region. The shift from one trap level to another may be the source of the side peaks in the spectrum.[37] LED M2 (with AlGaP EBL) and LED M3 (with graded AlGaP EBL) lead to stronger carrier confinement and carrier injection into the active region, resulting in a higher radiative recombination rate and more intense emission.

The summarized peak efficiencies and efficiency droops are shown in Table 1.

Table 1. Summarized parameters and corresponding results.

LEDs	Peak IQE (%)	Droop (%)
LED M1	95.2	13.4
LED M2	96	11.1
LED M3	96.3	9.4

The imbalance in the transport, confinement, or recombination behavior of electrons and holes in light-emitting devices, is known as carrier asymmetry in semiconductor devices. Carrier asymmetry describes these differences in behavior between the two types of carriers. The electron concentration profile of LED M1, LED M2, and LED M3 at 3 kA/cm^2 is shown in Fig. 3(a).

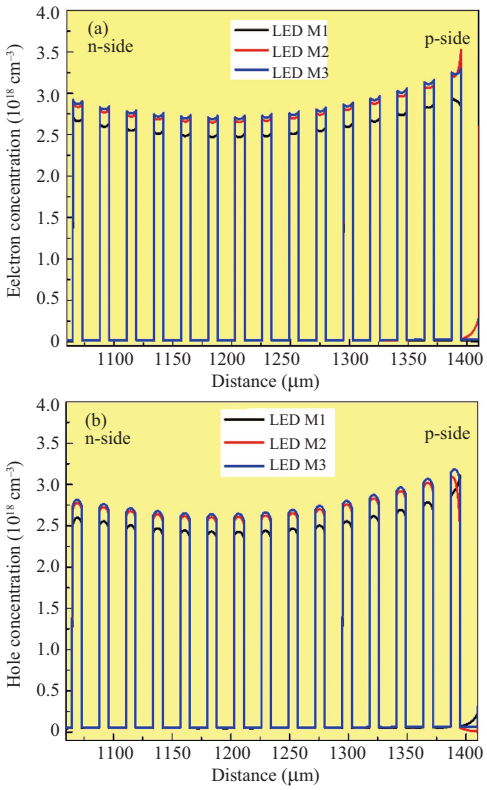


Fig. 3. (a) Electron concentration and (b) hole concentration of LED M1, LED M2, and LED M3 at 3 kA/cm^2.

Electrons have a smaller effective mass and are more mobile than holes. Thus, electrons can sweep into the p-region and contribute to non-radiative recombination in LED M1.[38] Ternary AlGaP EBL (LED M2) and GEBL (LED M3) improve the carrier distribution in MQWs. Improved electron confinement leads to increased electron concentration in the active zone of LED M3 in comparison to LED M1 and LED M2. As shown in Fig. 3(b), LED M3 significantly improves the hole concentration in the quantum well compared to LED M1 because the holes are heavy and less mobile indicating that more radiative recombination occurs. The findings indicate that with the addition of AlGaP EBL and GEBL, the hole concentration in the active region is higher than in LED M1.

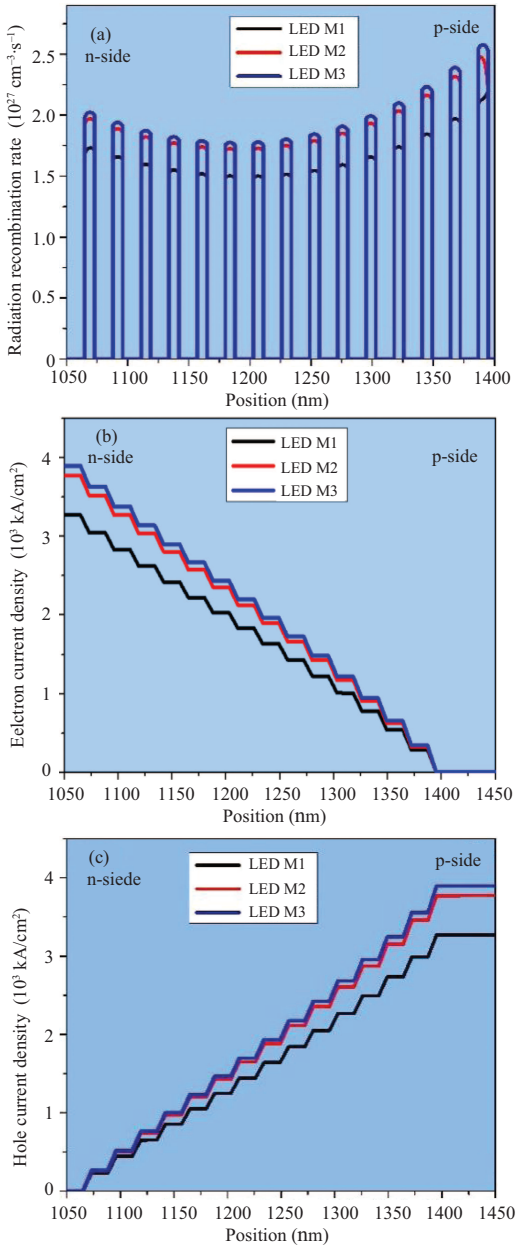


Fig. 4. (a) The radiative recombination rate, (b) the electron flux, and (c) the hole flux *versus* position graphs of LED M1, LED M2, and LED M3 at 3 kA/cm^2.

The radiative recombination profiles for LED M1, LED M2 as well as LED M3 are displayed in Fig. 4(a). Carrier asymmetry is reduced which promotes electron and hole

recombination.[39] Thus, the radiative recombination rate increases in LED M2 and LED M3. Improved carrier confinement results in improved radiative recombination in the active zone of LED M2 and LED M3. LED M3 exhibits 16% and 3.2% higher radiative recombination rate than LED M1 and LED M2 respectively. The u-shaped spread of radiative recombination rate is due to the asymmetric electron and hole concentration (as shown in Fig. 3). The u-shape distribution of hole concentration in Fig. 3(b) dominates the spread of the radiative recombination rate in the active region.

Figure 4(b) displays the electron current densities in the active areas of the three LEDs. The electron flux density represents electron current distribution. Thus, LED M3 (graded AlGaP EBL) has the highest injection and confinement of electrons in comparison to LED M1 and LED M2. Figure 4(c) shows hole current densities. The lower valence band height allows the holes to enter effectively into MQWs in LED M3 as compared to LED M1 and LED M2. Thus, in LED M3, hole flux is increased than LED M2 and LED M1.

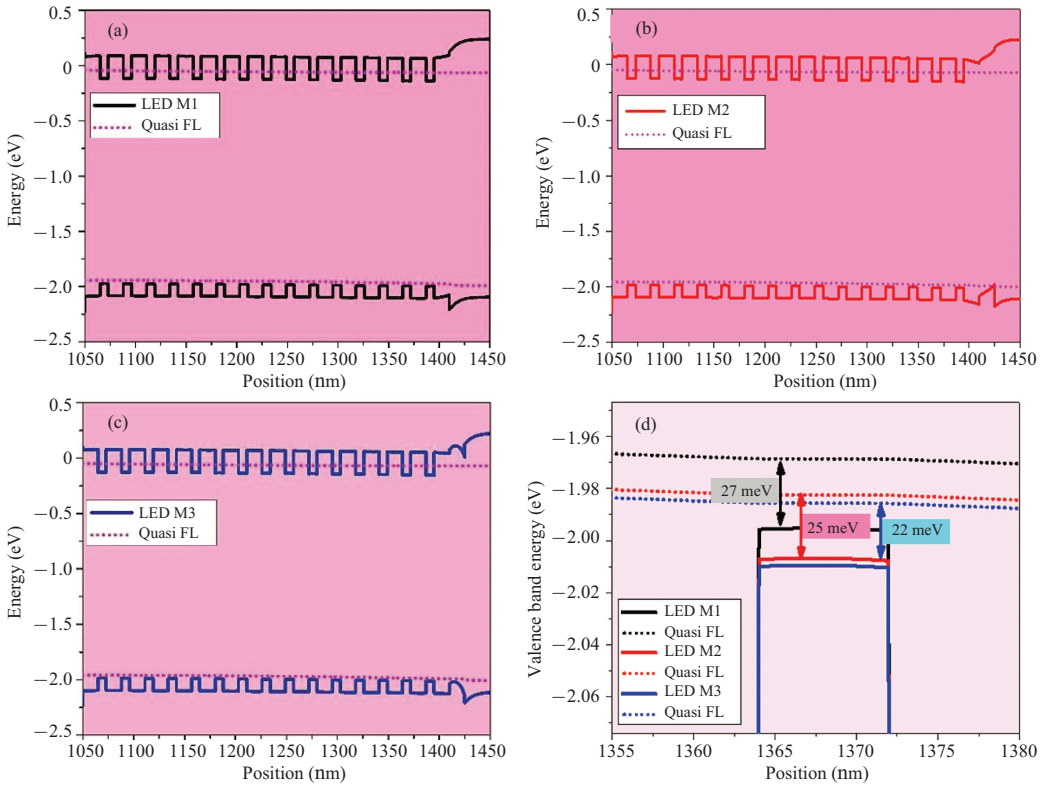


Fig. 5. Energy band diagrams of (a) LED M1, (b) LED M2, (c) LED M3, and (d) enlarged valence band diagram *versus* position plots of LED M1, LED M2, and LED M3 at 3 kA/cm^2.

Figures 5(a)–5(c) show the energy band diagrams for LED M1, LED M2, and LED M3. For an electron (hole), the potential barrier height is defined as the difference between the quasi-Fermi energy level (E_{fi}) and the conduction (valence) band level, i.e., E_c and E_v. To reduce the electron overflow, LED M2 utilizes AlGaP EBL on the p-side of the structure. The potential barrier heights (E_{fi}–E_v) in LED M2 increase with the use of ternary AlGaP EBL, increasing the concentration of carriers in the active zone. The ternary AlGaP EBL, therefore, does a better job of retaining carriers inside the active regions of LED M2. The ternary AlGaP EBL valence barrier height in LED M2 also leads to improvement in its hole concentration. In the figure, LED M3 (graded AlGaP EBL) further reduces the valence barrier height and improves hole injection compared with LED M1 and LED M2. Figure 5(d) shows the enlarged valence band diagram of LED M1, LED M2, and LED M3. The effective barrier height energy drops for hole injection in AlGaP EBLs, as seen in Fig. 5(d), which is advantageous for hole injection. LED M1, LED M2, and LED M3 have valence band and Fermi level differences of 27 meV, 25 meV, and 22 meV, respectively. As a result, the MQWs can effectively receive holes, improving the performance of LED M3 over LED M1 and LED M2. The absence of polarization fields in the III–phosphide material provides the comparatively flat band profile throughout the MQWs, as shown in Fig. 5. This flatness indicates effective carrier confinement within the active zone. The zinc-blende crystal structure of the III–phosphides (i.e., AlGaInP and AlGaP) employed in our device results in low polarization fields.

4. Conclusion

The effects of AlGaP EBLs on III–phosphide LEDs were examined. LEDs with AlGaP EBLs show a significant reduction in efficiency droop and produce light at $\sim$ 650 nm (peak).

We found that adding a ternary AlGaP EBL as well as graded-composition AlGaP EBL to the traditional LED results in better hole injection and device output. Thus, our device engineering and optimization of red AlGaInP-based LEDs exhibit a promising approach to achieve high performance. We believe our simpler approach is scalable at the industrial level as well.

Acknowledgement

The authors are obliged to Ghulam Ishaq Khan Institute of Engineering Sciences and Technology (Pakistan) for providing the needed resources for this research.

References

[1] Vanderwater D, Tan I H, Hofler G, Defevere D and Kish F A 1997 *Proc. IEEE* **85** 1752
[2] Tsao J Y, Crawford M H, Coltrin M E, Fischer A J, Koleske D D, Subramania G S, *et al.* 2014 *Adv. Opt. Mater.* **2** 809
[3] Gessmann T and Schubert E 2004 *J. Appl. Phys.* **95** 2203
[4] Vurgaftman I, Meyer J and Ram-Mohan L 2001 *J. Appl. Phys.* **89** 5815
[5] Cheng W C, Huang S Y, Chen Y J, Wang C S, Lin H Y, Wu T M, *et al.* 2018 *Sci. Rep.* **8** 911
[6] Guo X, Liu Q L, Tian H J, Guo C W, Li C, Hu A Q, *et al.* 2018 *Chin. Phys. B* **27** 098502
[7] Yadav A, Titkov I E, Sokolovskii G S, Karpov S Y, Dudelev V V, Soboleva K K, *et al.* 2018 *J. Appl. Phys.* **124** 013103
[8] Oh H S, Park S H, Kim Y J, Lee H J and Cho Y D 2013 *Asia Commun. Photon. Conf.* AF2K5
[9] Shim J I, Han D P, Kim H, Shin D S, Lin G B, Meyaard D S, *et al.* 2012 *Appl. Phys. Lett.* **100** 111106
[10] Royo P, Stanley R P, Ilegems M, Streubel K P, Moser M and Gulden K H 2001 *Proc. SPIE* **4278** 61
[11] Kish F A and Fletcher R M 1997 *AlGaInP Light-Emitting Diodes, in Semiconductors and Semimetals*, eds. Stringfellow G B and Craford M G, Chapter 5, Vol. 48 (Amsterdam: Elsevier) pp. 149–C3
[12] Altieri P, Jaeger A, Windisch R, Linder N, Stauss P, Oberschmid R, *et al.* 2005 *J. Appl. Phys.* **98** 086101
[13] Cho J, Schubert E F and Kim J K 2013 *Laser Photon. Rev.* **7** 408
[14] Lin X, Liu D, Lin G, Zhang Q, Gao N, Zhao D, *et al.* 2014 *RSC Adv.* **4** 63143
[15] Streubel K, Linder N, Wirth R and Jaeger A 2002 *IEEE J. Sel. Top. Quantum Electron.* **8** 321
[16] Su J Y, Wu M C, Chen W B and Su Y K 2003 *IEEE Electron Dev. Lett.* **24** 159
[17] Park C, Park K, Jang S, Yu J and Lee Y 2010 *Semicond. Sci. Technol.* **25** 085012
[18] Anum M, Usman M, Habib U and Ali S 2024 *Phys. Scr.* **99** 0659
[19] Zhang A, Yao J, Xing Z, Wang F, Liou J J and Liu Y 2025 *Opt. Eng.* **64** 027103
[20] Lee H, Lee D, Song Y, Lee Y and Yu J 2011 *Solid-State Electron.* **56** 79
[21] Fedorova O A, Bulashevich K A and Karpov S Y 2021 *Opt. Express* **29** 35792
[22] Oh C H, Shim J I and Shin D S 2019 *Jpn. J. Appl. Phys.* **58** SCCC08
[23] Zhang Y, Lu S, Liu B, Gao H, Zhou Y, Fang W, *et al.* 2025 *IEEE Trans. Electron Dev.* **72** 2769
[24] Wang Y, Wang B, Sasangka W A, Bao S, Zhang Y, Demir H V, *et al.* 2018 *Photon. Res.* **6** 290
[25] Boyer J T, Lepkowski D L, Chmielewski D J and Grassman T J 2019 *Sol. Energy Mater. Sol. Cells* **202** 110133
[26] Tremblay R, Burin J P, Rohel T, Gauthier J P, Almosni S, Quinci T, *et al.* 2017 *J. Cryst. Growth* **466** 6
[27] Piskorski L, Sarzala R P and Nakwaski W 2007 *Semicond. Sci. Technol.* **22** 593
[28] Wang C 2017 *Epitaxy and Characterization of AlGaInP-Based LEDs on Si Substrates for Visible-Spectrum Light Emission* (Singapore: Nanyang Technol. Univ., Sch. Electr. Electron. Eng.)
[29] Chang S J, Chang C, Su Y, Chang P, Wu Y, Huang K, *et al.* 1997 *IEE Proc.-Optoelectron.* **144** 405
[30] Rabinovich O, Gostischev P, Sizov S, Orlova M, Didenko S, Osipov Y, *et al.* 2019 *Proc. Manuf.* **37** 195
[31] Zhu D 2011 *Investigating and Optimizing Carrier Transport, Carrier Distribution, and Efficiency Droop in GaN-Based Light-Emitting Diodes* (Troy, NY: Rensselaer Polytech. Inst.)
[32] Piprek J 2007 *Nitride Semiconductor Devices: Principles and Simulation* (Hoboken, NJ: John Wiley & Sons)
[33] Chuang S and Chang C K 1996 *Phys. Rev. B* **54** 2491
[34] Bulashevich K, Khokhlev O, Evstratov I Y and Karpov S Y 2012 *Proc. SPIE* 8278 82780F
[35] Sabathil M, Laubsch A and Linder N 2007 *Proc. SPIE* **6486** 64860V
[36] Yadav A, Titkov I E, Sokolovskii G S, Karpov S Y, Dudelev V V, Soboleva K K, *et al.* 2016 *Proc. SPIE* **9768** 97680M
[37] Peng D and Liu K 2021 *J. Phys.: Conf. Ser.* **1865** 012003
[38] Wang G, Yi X, Zhan T and Huang Y 2019 *The AlGaInP/AlGaAs Material System and Red/Yellow LED, in Light-Emitting Diodes: Materials, Processes, Devices and Applications*, edd. Li J and Zhang G Q (Cham: Springer Int. Publ.) pp. 171–202
[39] Park J H, Lee J W, Kim D Y, Cho J, Schubert E F, Kim J, *et al.* 2016 *J. Appl. Phys.* **119** 055705